NHE3-dependent cytoplasmic alkalinization is triggered by Na+-glucose cotransport in intestinal epithelia

Jerrold R. Turner and Eric D. Black

Am J Physiol Cell Physiol 281:1533-1541, 2001.

AJP - Cell Physiology is dedicated to innovative approaches to the study of cell and molecular physiology. It is published 12 times a year (monthly) by the American Physiological Society, 9650 Rockville Pike, Bethesda MD 20814-3991. ISSN: 0363-6143, ESSN: 1522-1563. Visit our website at http://www.the-aps.org/.

Am J Physiol Cell Physiol
281: C1533–C1541, 2001.

NHE3-dependent cytoplasmic alkalinization is triggered by Na^+-glucose cotransport in intestinal epithelia

JERROLD R. TURNER AND ERIC D. BLACK
Department of Pathology, Wayne State University School of Medicine, Detroit, Michigan 48201

Received 5 February 2001; accepted in final form 6 July 2001

Turner, Jerrold R., and Eric D. Black. NHE3-dependent cytoplasmic alkalinization is triggered by Na^+-glucose cotransport in intestinal epithelia. *Am J Physiol Cell Physiol* 281: C1533–C1541, 2001.—Cytoplasmic pH (pH_i) was evaluated during Na^+-glucose cotransport in Caco-2 intestinal epithelial cell monolayers. The pH_i increased by 0.069 ± 0.002 within 150 s after initiation of Na^+-glucose cotransport. This increase occurred in parallel with glucose uptake and required expression of the intestinal Na^+-glucose cotransporter SGLT1. S-3226, a preferential inhibitor of Na^+/H^+ exchanger (NHE) isoform 3 (NHE3), prevented cytoplasmic alkalinization after initiation of Na^+-glucose cotransport with an ED_{50} of 0.35 μM, consistent with inhibition of NHE3, but not NHE1 or NHE2. In contrast, HOE-694, a poor NHE3 inhibitor, failed to significantly inhibit pH_i increases at <500 μM. Na^+-glucose cotransport was also associated with activation of p38 mitogen-activated protein (MAP) kinase, and the p38 MAP kinase inhibitors PD-169316 and SB-202190 prevented pH_i increases by 100 ± 0.1 and 86 ± 0.1%, respectively. Conversely, activation of p38 MAP kinase with anisomycin induced NHE3-dependent cytoplasmic alkalinization in the absence of Na^+-glucose cotransport. These data show that NHE3-dependent cytoplasmic alkalinization occurs after initiation of SGLT1-mediated Na^+-glucose cotransport and that the mechanism of this NHE3 activation requires p38 MAP kinase activity. This coordinated regulation of glucose (SGLT1) and Na^+ (NHE3) absorptive processes may represent a functional activation of absorptive enterocytes by luminal nutrients.

SGLT1; p38 mitogen-activated protein kinase; nutrient absorption; Na^+/H^+ exchanger isoform 3

IN THE MAMMALIAN SMALL INTESTINE, Na^+ absorption provides the driving force for transcellular absorption of glucose and many amino acids. Deficiency of the apical Na^+-glucose cotransporter SGLT1 in humans leads to glucose/galactose malabsorption, with severe diarrhea and dehydration (21). Similarly, a genetically engineered mouse lacking functional Na^+/H^+ exchanger isoform 3 (NHE3) suffers from diarrhea, intestinal malabsorption, dehydration, mild acidosis, and increased volume and alkalinity of the intestinal contents (16). Thus loss of NHE3, the primary Na^+ absorptive pathway in the intestine and renal tubules, leads to fluid and pH imbalances (16, 27). Conversely, increased renal tubular NHE3 activity has been suggested as a disease mechanism in spontaneously hypertensive rats (3), perhaps because of increased Na^+ and volume retention.

Recently, NHE3 regulation has been the subject of intense investigation. For example, it is clear that NHE3 activity can be acutely increased by recruitment of NHE3 from intracellular stores to the plasma membrane (1, 6). NHE3 can also be regulated by the actin cytoskeleton (8, 18), an effect at least partly mediated by a family of Na^+/H^+ exchanger regulatory factors (26, 28) that interact with NHE3 and cytoskeletal proteins. In renal thick ascending limb, NHE3 can also be activated by hyposmolality (25).

Although NHE3 is highly enriched in the brush border of small intestinal absorptive (villus) enterocytes (4), only one study has examined coordination of NHE3 activity with the activity of absorptive pathways. This study demonstrated preferential activation of apical Na^+/H^+ exchange after cytoplasmic acidification induced by apical H^+-solute cotransport (19). This led to the conclusion that activation of apical Na^+/H^+ exchange by H^+-solute cotransport resulted in optimal absorption of Na^+ and nutrients in conjunction with maintenance of intracellular pH (pH_i) (19). Such regulation is likely critical in absorptive epithelia, inasmuch as it is a necessary component of cell volume and ion channel regulatory pathways (11, 12, 15).

We recently developed an in vitro model of intestinal Na^+-glucose cotransport using Caco-2 cells stably transfected with intestinal SGLT1 (24). We showed that monolayers of these cells are capable of vectorial Na^+-glucose cotransport with kinetic properties similar to those observed in native small intestine (23, 24). Moreover, like native small intestinal mucosae, monolayers of these cells regulate paracellular transport after activation of SGLT1-mediated Na^+-glucose cotransport (24). Further characterization of the signaling mechanisms necessary for this process demonstrated that, in the presence of ongoing Na^+-glucose cotransport, inhibition of NHE3 prevented SGLT1-dependent regulation of paracellular permeability (22). Thus we hypothesized that SGLT1- and NHE3-mediated transcellular transport might be coordinately regulated.

Address for reprint requests and other correspondence: J. R. Turner, Dept. of Pathology, The University of Chicago, 5841 S. Maryland Ave., MC 1089, Chicago, IL 60637 (E-mail: jturner@bsd.uchicago.edu).

The costs of publication of this article were defrayed in part by the payment of page charges. The article must therefore be hereby marked "*advertisement*" in accordance with 18 U.S.C. Section 1734 solely to indicate this fact.

The goal of these studies was to determine whether a functional interaction exists between SGLT1 and NHE3. Our studies show that initiation of SGLT1-dependent Na^+-glucose cotransport leads to cytoplasmic alkalinization and that this alkalinization is dependent on NHE3. Moreover, the data suggest that p38 mitogen-activated protein (MAP) kinase is a critical intermediate in this SGLT1-dependent NHE3 activation.

METHODS

Materials. Tissue culture media and serum were obtained from GIBCO (Life Technologies, Gaithersburg, MD). HOE-694 and S-3226 were the kind gifts of Dr. Hans-Jochen Lang (Hoechst-Marion Roussel) (2, 17). Other Na^+/H^+ exchange inhibitors were obtained from Sigma (St. Louis, MO). The rho kinase inhibitor Y-27632 was generously provided by Yoshitomi Pharmaceutical Industries (Saitama, Japan).

Cell culture. Clonal populations of Caco-2 cells with active physiological Na^+-glucose cotransport were generated by stable transfection with native intestinal SGLT1 and maintained in high-glucose (25 mM) DMEM with 10% fetal calf serum, 15 mM HEPES, pH 7.4, and 0.25 mg/ml geneticin, as described previously (23). For fluorometry, cells from a confluent flask were lightly trypsinized, replated onto collagen-coated coverslips, and used at 100% confluence after 4–5 days. For p38 MAP kinase assays, cells were grown to confluence in 35-mm-diameter tissue culture dishes (Corning-Costar). Whether grown on coverslips or tissue culture dishes, cells were cultured in low-glucose (5.5 mM) DMEM supplemented with 19.5 mM mannitol (to maintain overall osmolarity), 10% fetal calf serum, and 15 mM HEPES, pH 7.4 (without geneticin), for 18 h before use in experiments. All experiments were performed in nominally HCO_3^--free Hanks' balanced saline solution containing 25 mM sugar (glucose or mannose, to maintain overall osmolarity) and 15 mM HEPES.

Sugar uptake assays. Sugar uptake assays were done in triplicate using cells grown on collagen-coated 1.9-cm^2 surface area tissue culture dishes (Corning-Costar). Briefly, wells were washed three times with glucose-free medium, incubated for 15 min at 37°C with glucose-free medium containing the drugs indicated, and then incubated for the indicated time at 37°C with 0.4 ml of glucose-free medium containing ^{14}C-labeled α-D-methyl glucoside (23) and the indicated drugs. For the assays evaluating drug inhibitions (see Fig. 8), uptake was determined after 15 min of incubation in glucose-free medium containing ^{14}C-labeled α-D-methyl glucoside. Wells were then washed at 4°C in medium with 25 mM glucose, and cells were solubilized with 0.1 ml of 0.1 N NaOH. Specificity was confirmed by >97% reduction in ^{14}C-labeled α-D-methyl glucoside uptake when 0.1 mM phloridzin was added and by >98% reduction when 10 mM glucose was added.

Measurement of pH_i. Confluent monolayers were washed with medium (with 25 mM mannose) and incubated for 15 min at room temperature with 3.5 μM 2′,7′-bis(2-carboxyethyl)-5(6)-carboxyfluorescein acetoxymethyl ester (Molecular Probes, Eugene, OR). After they were washed, 2′,7′-bis-(2-carboxyethyl)-5(6)-carboxyfluorescein-loaded cells were warmed to 37°C and analyzed using a fluorometer equipped with dual emission/excitation monochromators (model RC-M, Photon Technology International, Monmouth Junction, NJ). Fluorescence was measured at excitations of 439 and 502 nm and emission of 535 nm. Fluorometric ratios corresponding to pH 7.00, 7.25, 7.50, and 7.75 were determined by clamping pH_i using medium (at the designated pH) containing 110 mM KCl (in place of NaCl) and 10 μg/ml nigericin. Standard values were obtained for each sample set, and standard curves were generated and experimental data were analyzed using Felix software (version 1.21, Photon Technology International). Initial pH_i values averaged 7.48 ± 0.005. Unless otherwise indicated, drugs were added in medium containing 25 mM mannose 15 min before exchange for medium containing 25 mM glucose and the drug. LY-294002, wortmannin, and ML-7 were added 30 min before the pH response to glucose was tested, cytochalasin D was added 3 h before the pH response to glucose was tested, and cells were preloaded with phalloidin for 18 h before the pH response to glucose was tested.

Immunoblot and in vitro p38 MAP kinase activity assay. Confluent monolayers were preincubated in medium with 25 mM mannose and 0.5 mM phloridzin for 20 min at 37°C. The buffer was then exchanged isosmotically for medium with 25 mM glucose at 37°C. After incubation at 37°C for the times indicated, cells were rapidly rinsed with PBS at 4°C and lysed in 0.4 ml of lysis buffer (20 mM Tris, 150 mM NaCl, 1 mM EDTA, 1 mM EGTA, 1% Triton X-100, 2.5 mM sodium pyrophosphate, 1 mM β-glycerophosphate, 1 mM Na_3VO_4, 1 μg/ml leupeptin, and 1 mM phenylmethylsulfonyl fluoride, pH 7.5). After incubation on ice for 5 min, lysates were centrifuged at 14,000 *g* for 10 min, and supernatants were used for subsequent assays. Protein content was determined using the bicinchoninic acid protein assay (Pierce Chemical, Rockford, IL).

For immunoblot determination of p38 MAP kinase diphosphorylation, samples were separated on 10% SDS-polyacrylamide gels and transferred to polyvinylidene difluoride membranes. Duplicate gels were immunoblotted with monoclonal antisera to diphosphorylated p38 MAP kinase (New England BioLabs, Beverly, MA) or total p38 MAP kinase (Santa Cruz Biotechnology, Santa Cruz, CA). Antibody binding was detected with affinity-purified goat anti-mouse IgG peroxidase-conjugated antibodies (ICN, Costa Mesa, CA) and chemiluminescence on preflashed BioMax MR film (Eastman Kodak). Signal intensity, corrected for background, was determined by densitometry using SigmaGel software (SPSS, Chicago, IL).

In vitro p38 MAP kinase activity was determined using a kit purchased from New England BioLabs. Duplicate 200-μg aliquots of cell lysates were incubated with excess immobilized anti-p38 antisera. Immunoprecipitated p38 MAP kinase was then resuspended in 50 μl of kinase assay buffer (25 mM Tris, 5 mM β-glycerophosphate, 2 mM dithiothreitol, 0.1 mM Na_3VO_4, and 10 mM $MgCl_2$, pH 7.5) with 2 μg of an ATF-2 fusion protein (containing residues 19–96 of ATF-2) and 0.2 mM ATP. After 30 min at 30°C the reaction was terminated by the addition of 25 μl of 3× SDS-PAGE sample buffer. Preliminary experiments showed that these incubation conditions were within the linear range of the assay. Phosphorylation of ATF-2 was determined by immunoblot, as described above, using a rabbit polyclonal antibody that specifically reacts with ATF-2 phosphorylated at threonine-71.

Statistical analysis. All experiments were performed multiple times with two or more samples in each individual experiment. Results are expressed as means ± SE. Conditions were compared using Student's *t*-test (Excel, Microsoft, Redmond, WA). In pH_i experiments, the change in pH_i at 120 s after buffer exchange was compared using Student's *t*-test, and pH_i response curves over the interval from 0 to 300 s were compared by analysis of variance (SigmaStat, SPSS).

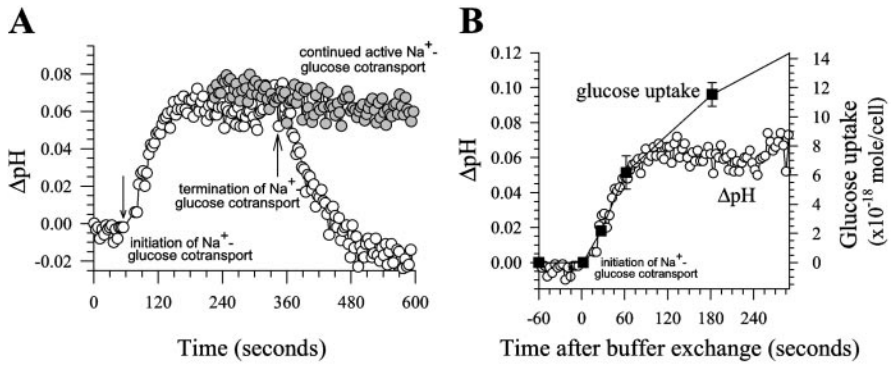

Fig. 1. Reversible increases in cytoplasmic pH (pH_i) after initiation of Na^+-glucose cotransport occur in parallel with glucose uptake. *A*: 2′,7′-bis(2-carboxyethyl)-5(6)-carboxyfluorescein (BCECF)-loaded SGLT1-transfected Caco-2 cells were incubated in medium containing 25 mM mannose and 0.5 mM phloridzin. Initiation of Na^+-glucose cotransport by exchange of this buffer for medium containing 25 mM glucose in place of mannose and phloridzin (arrow) resulted in pH_i increases that stabilized within 150 s to a new pH_i that was 0.069 ± 0.002 pH units greater than the initial value. Subsequent termination of Na^+-glucose cotransport by exchange back into medium containing 25 mM mannose and 0.5 mM phloridzin (open circles) resulted in a decrease in pH_i to values that were comparable to initial values, whereas pH_i remained elevated as long as Na^+-glucose cotransport continued (shaded circles). Values are means from 3 independent experiments. *B*: SGLT1-dependent glucose uptake (squares) compared with pH_i (from *A*). Although SGLT1-dependent glucose uptake was linear at >60 s, initial rates were more rapid and paralleled alkalinization of pH_i. SGLT1-dependent glucose uptake was determined as phloridzin-insensitive uptake of ^{14}C-labeled α-D-methyl glucoside. Values are means ± SE of triplicate wells at each time point.

RESULTS

Cytoplasmic alkalinization occurs rapidly after Na^+-glucose cotransport. The Caco-2 cell line used for these studies was stably transfected with the native intestinal Na^+-glucose cotransporter SGLT1. We previously showed that these cells take up sugar with kinetics typical for native SGLT1 and that the transfected native SGLT1 is appropriately localized to the apical membrane domain in polarized monolayers (23). Such monolayers demonstrate vectorial Na^+ and glucose transport, which coincides with the development of an Na^+-dependent short-circuit current (24). We have also shown that these cells express all three intestinal Na^+/H^+ exchanger isoforms: basolateral NHE1 and apical NHE2 and NHE3 (22).

To evaluate the potential for a functional interaction between Na^+/H^+ exchange and Na^+-glucose cotransport, we first evaluated pH_i during initiation and termination of Na^+-glucose cotransport (Fig. 1). Initiation of SGLT1-mediated Na^+-glucose cotransport (by isosmotic substitution of mannose with glucose) resulted in a rapid pH_i increase of 0.069 ± 0.002 that was complete within 150 s ($P < 0.001$). The pH_i was then stable at this new elevated level for ≥30 min, as long as Na^+-glucose cotransport continued. Inhibition of SGLT1-mediated Na^+-glucose cotransport caused pH_i to rapidly return to values approximating those before initiation of Na^+-glucose cotransport (Fig. 1*A*). The nonmetabolizable glucose analog α-D-methyl glucoside that is transported by SGLT1 elicited similar pH_i increases (Fig. 2), suggesting that SGLT1-mediated Na^+-glucose cotransport was necessary but that metabolism of the transported carbohydrate was not. Moreover, although SGLT1-mediated Na^+-glucose cotransport and intracellular accumulation of glucose continued well after pH_i stabilized at the new steady-state value, α-D-methyl glucoside uptake at early time points paralleled pH_i increases (Fig. 1*B*). Further evidence that the observed cytoplasmic alkalinization required SGLT1 is provided by analysis of a separate clone of nontransfected Caco-2 cells that do not express SGLT1. These cells did not exhibit changes in pH_i after isosmotic exchange into buffer with glucose. Finally, pH_i increases in SGLT1-expressing Caco-2 were not an

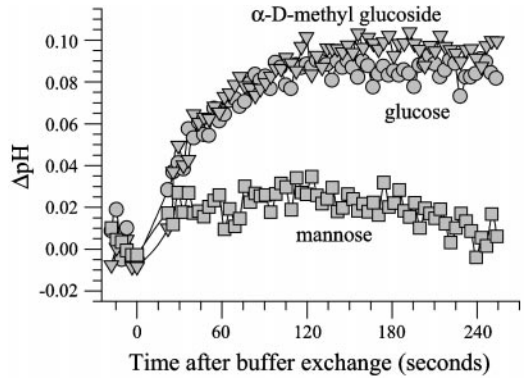

Fig. 2. Cytoplasmic alkalinization requires SGLT1-mediated Na^+-glucose cotransport. BCECF-loaded SGLT1-transfected Caco-2 cells were incubated in medium containing 25 mM mannose and 0.5 mM phloridzin. Exchange of mannose-phloridzin medium for medium containing 25 mM glucose (circles) resulted in a rapid and sustained rise in pH_i (see Fig. 1). Similarly, exchange into medium with 25 mM α-D-methyl glucoside, a nonmetabolizable glucose analog, caused a similar rapid and sustained rise in pH_i (inverted triangles). In contrast, exchange of medium containing 25 mM mannose and 0.5 mM phloridzin for medium containing 25 mM mannose, but no phloridzin, resulted in only a small transient pH change (squares), presumably due to the physical stimulus of the buffer exchange. Values are representative of ≥3 experiments, all with similar results.

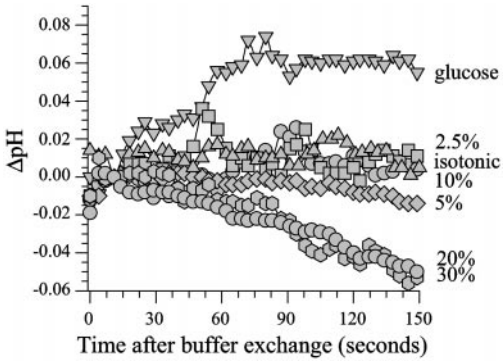

Fig. 3. Cytoplasmic alkalinization does not occur after hypotonic cell swelling. BCECF-loaded SGLT1-transfected Caco-2 cells were incubated in medium containing 25 mM mannose and 0.5 mM phloridzin. Exchange of the mannose-phloridzin medium for medium containing 25 mM glucose resulted in a rapid and sustained rise in pH_i (see Fig. 1). In contrast, exchange of the medium with 25 mM mannose and 0.5 mM phloridzin for isotonic medium with 25 mM mannose or the same medium diluted by 2.5, 5, 10, 20, or 30% with water did not cause significant cytoplasmic alkalinization and, at greater dilutions, caused cytoplasmic acidification. Values are representative of ≥3 experiments, all with similar results.

artifact due to washout of the SGLT1 inhibitor phloridzin, since exchange into medium with mannose, but without phloridzin or glucose, did not induce significant alkalinization (Fig. 2).

Although all buffers used for these studies were osmotically balanced, SGLT1-mediated uptake of Na^+ and glucose has been shown to cause cell volume increases of 4% within 30 s in isolated villus enterocytes (10). Quantitatively similar volume increases can be induced by 5% hypotonic medium (11). However, swelling in 2.5, 5, or 10% hypotonic media in the absence of Na^+-glucose cotransport did not cause significant changes in pH_i (Fig. 3). Moreover, greater degrees of cell swelling induced by 20–30% hypotonic media caused cytoplasmic acidification. Thus the pH_i increases observed after Na^+-glucose cotransport cannot be simply explained by cell swelling.

Na^+-glucose cotransport-dependent alkalinization requires NHE3 but not NHE1 or NHE2. As summarized above, our previous data led to the hypothesis that Na^+/H^+ exchange might be activated after Na^+-glucose cotransport (22). The observation that pH_i increases after initiation of Na^+-glucose cotransport is consistent with activation of Na^+/H^+ exchange. Because we previously showed that the Caco-2 cells used in this study express all three intestinal Na^+/H^+ exchanger isoforms (22), we sought to determine which, if any, of the Na^+/H^+ exchangers were responsible for the observed increases in pH_i. We compared the effects of two Na^+/H^+ exchange inhibitors, S-3226 and HOE-694, on pH_i increases after initiation of Na^+-glucose cotransport. S-3226 has been reported to inhibit NHE3 with an IC_{50} of 0.02 μM (human NHE3 expressed in fibroblasts) or 0.2 μM (porcine kidney brush-border preparations) (17). In contrast, S-3226 inhibits NHE1 and NHE2 relatively poorly, with IC_{50} of 3.5 μM for NHE1 and 80 μM for NHE2 (17). At 0.1 μM, S-3226 prevented alkalinization after Na^+-glucose cotransport by 41 ± 8% ($P < 0.03$), while 1 μM S-3226 prevented alkalinization by 66 ± 1% ($P < 0.001$; Fig. 4). Further inhibition was not apparent at higher S-3226 concentrations. If a linear relationship between the inhibitory effects of S-3226 at 0.1 and 1 μM is assumed, these data correspond to an ED_{50} of 0.35 μM, a value comparable to the IC_{50} of 0.2 μM reported for NHE3 from porcine kidney brush-border preparations (17). Thus pharmacological inhibition of NHE3 can prevent the majority of cytoplasmic alkalinization after Na^+-glucose cotransport.

Because S-3226 was not able to completely prevent cytoplasmic alkalinization after Na^+-glucose cotransport, we considered the possibility that NHE1 or NHE2 might be responsible for the remaining small amount of alkalinization. To evaluate the roles of NHE1 and NHE2 in cytoplasmic alkalinization after Na^+-glucose cotransport, we used the inhibitor HOE-694 (2). This agent preferentially inhibits NHE1 and NHE2 with IC_{50} values of 0.16 and 5 μM, respectively, while NHE3 is inhibited poorly (IC_{50} = 650 μM). HOE-694 at ≤100 μM did not significantly inhibit cytoplasmic alkalinization after initiation of Na^+-glucose cotransport (P 0.05; Fig. 5). However, at 500 μM, which partially inhibits NHE3, HOE-694 prevented cytoplasmic alkalinization by 50 ± 5% ($P < 0.03$). Thus these data suggest that neither NHE1 nor NHE2 is involved in the pH_i regulation that follows initiation of Na^+-glucose cotransport. Moreover, together with the S-3226 inhibitor data, the results using HOE-694 show that NHE3 is the Na^+/H^+ exchanger isoform required for cytoplasmic alkalinization after initiation of Na^+-glucose cotransport. Finally, to further characterize the role of NHE3 in these pH_i increases, we evaluated the rate of cytoplasmic alkalinization in the first 60 s after initiation of Na^+-glucose cotransport. During the first 60 s after exchange into medium with 25 mM glucose, the rate of NHE3-dependent alkalinization increased by 0.42×10^{-3} pH unit/s (Fig. 6).

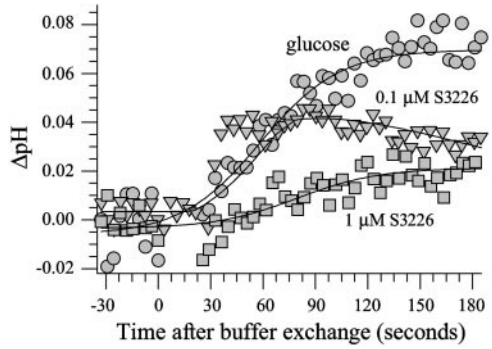

Fig. 4. Cytoplasmic alkalinization after initiation of Na^+-glucose cotransport is inhibited by S-3226. As shown in Figs. 1 and 2, exchange of medium containing 25 mM mannose for medium containing 25 mM glucose resulted in a rapid and sustained rise in pH_i (circles). Inclusion of the preferential NHE3 inhibitor S-3226 at 0.1 μM (inverted triangles) or 1 μM (squares) markedly inhibited this alkalinization. Values are representative of >5 experiments, all with similar results.

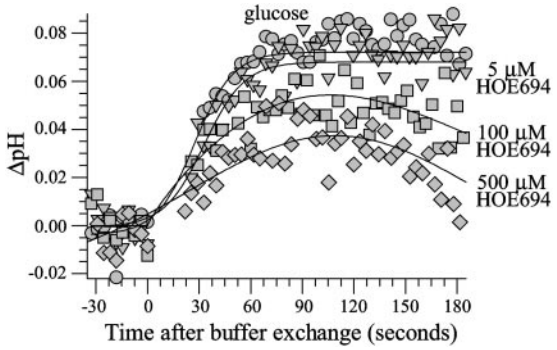

Fig. 5. Cytoplasmic alkalinization after initiation of Na^+-glucose cotransport is poorly inhibited by HOE-694. As shown in Figs. 1 and 2, exchange of medium containing 25 mM mannose for medium containing 25 mM glucose resulted in a rapid and sustained rise in pH_i (circles). Inclusion of the Na^+/H^+ exchange inhibitor HOE-694 at 5 μM (inverted triangles) did not significantly inhibit this alkalinization. Results with 50 μM HOE-694 were similar. A small but statistically insignificant degree of inhibition was seen with 100 μM HOE-694 (squares), which completely inhibits NHE1 and NHE2 but also slightly inhibits NHE3. Only 500 μM HOE-694 (diamonds), which inhibits NHE3, significantly inhibited cytoplasmic alkalinization after initiation of Na^+-glucose cotransport. Values are representative of >5 experiments, all with similar results.

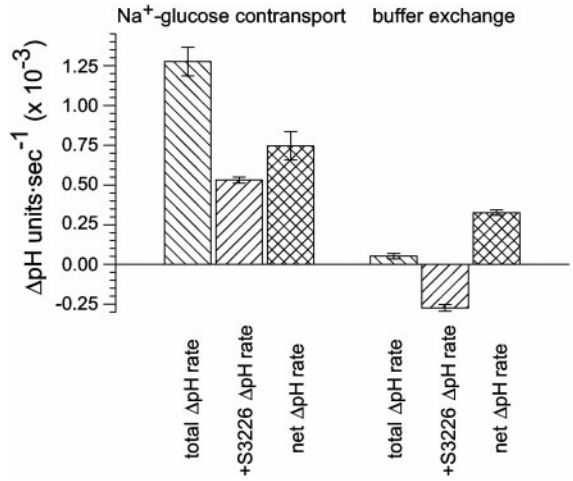

Fig. 6. Rate of NHE3-dependent cytoplasmic alkalinization is increased after initiation of Na^+-glucose cotransport. The rate of cytoplasmic alkalinization during the first 60 s after initiation of Na^+-glucose cotransport was determined by least-squares analysis of data from 3 separate experiments for each condition. To inhibit NHE1 and NHE2, all experiments were done in the presence of 50 μM HOE-694. Rates of cytoplasmic alkalinization after initiation of Na^+-glucose cotransport or a control buffer exchange (see Fig. 2) are indicated ("total ΔpH rate"). To determine the NHE3-dependent component of alkalinization, identical studies were performed in the presence of NHE3 inhibition with 5 μM S-3226 ("+S3226 ΔpH rate"). The difference between cytoplasmic alkalinization rates in the absence and presence of S-3226 was defined as the net NHE3-dependent cytoplasmic alkalinization rate ("net ΔpH rate"). The difference between the net ΔpH rate during the first 60 s after initiation of Na^+-glucose cotransport and the net ΔpH rate during the first 60 s after buffer exchange without initiation of Na^+-glucose cotransport was 0.42×10^{-3} pH unit/s. All comparisons between cells with and without Na^+-glucose cotransport were statistically significant ($P < 0.05$).

Cytoplasmic alkalinization can be prevented by p38 MAP kinase inhibitors. As shown above, hypotonic swelling did not cause pH_i increases comparable to those following Na^+-glucose cotransport. However, it is clear that cell volume increases after Na^+-glucose cotransport (10, 13). Thus we considered the hypothesis that activation of the osmotically responsive p38 MAP kinase could be involved in the NHE3-dependent cytoplasmic alkalinization after initiation of Na^+-glucose cotransport. Two separate structurally related p38 MAP kinase inhibitors, PD-169316 (5 μM) and SB-202190 (10 μM), inhibited cytoplasmic alkalinization after initiation of Na^+-glucose cotransport by 100 ± 0.1 and 86 ± 0.1%, respectively (Fig. 7; $P < 0.01$). In contrast, the structurally similar inactive compound SB-202474 (10 μM) did not affect cytoplasmic alkalinization after initiation of Na^+-glucose cotransport. Thus these data suggest that p38 MAP kinase may be an intermediate in the signal transduction pathway between Na^+-glucose cotransport and NHE3-dependent cytoplasmic alkalinization. Notably, the effects of p38 MAP kinase inhibitors and Na^+/H^+ exchange inhibitors on cytoplasmic alkalinization are not due to inhibition of Na^+-glucose cotransport, since none of the compounds used in these studies inhibited the Na^+-glucose cotransporter SGLT1 (Fig. 8).

p38 MAP kinase is rapidly activated after initiation of Na^+-glucose cotransport. We sought to confirm that activation of p38 MAP kinase did indeed follow the initiation of Na^+-glucose cotransport with a time course consistent with that of NHE3-dependent alkalinization. Intracellular activation of p38 MAP kinase is accomplished by the p38 MAP kinase kinase that phosphorylates p38 MAP kinase at threonine-180 and tyrosine-182. Thus immunoblot using antisera specific for the diphosphorylated form of p38 MAP kinase can be used to infer kinase activation. Such immunoblots showed a 3.7 ± 0.3-fold increase in diphosphorylated p38 MAP kinase (Fig. 9; $P < 0.01$). This was comparable to the 4.1 ± 0.2-fold increase in p38 MAP kinase

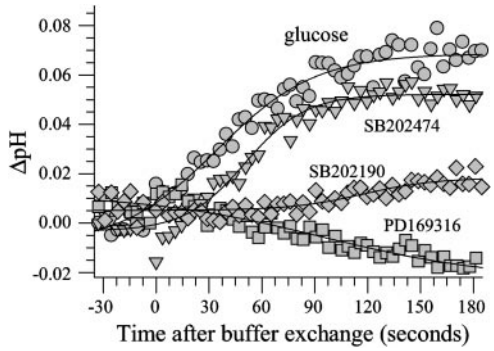

Fig. 7. Inhibition of p38 mitogen-activated protein (MAP) kinase prevents cytoplasmic alkalinization after initiation of Na^+-glucose cotransport. Exchange of medium containing 25 mM mannose for medium containing 25 mM glucose resulted in a rapid and sustained rise in pH_i (circles). Inclusion of the p38 MAP kinase inhibitors PD-169316 at 5 μM (squares) and SB-202190 at 10 μM (diamonds) effectively prevented cytoplasmic alkalinization. In contrast, the inactive control compound SB-202474 (10 μM) had no effect on cytoplasmic alkalinization after initiation of Na^+-glucose cotransport (inverted triangles). Values are representative of ≥5 experiments, all with similar results.

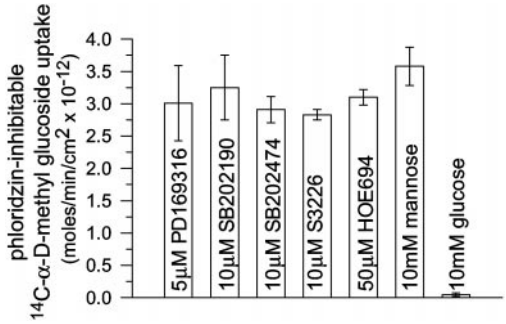

Fig. 8. Na^+/H^+ exchange inhibitors and p38 MAP kinase inhibitors do not affect Na^+-glucose cotransport. Na^+-glucose cotransport activity was assessed as uptake of 100 μM ^{14}C-labeled α-D-methyl glucoside, a glucose analog that is neither metabolized nor transported by the basolateral facilitated exchanger GLUT2. Thus ^{14}C-labeled α-D-methyl glucoside accumulates intracellularly after SGLT1-mediated Na^+-dependent uptake. We previously showed that, under the conditions used for these assays, uptake kinetics are linear with respect to time and correspond to those of intestinal SGLT1 (23). The drugs do not alter phloridzin-inhibitable ^{14}C-labeled α-D-methyl glucoside uptake. Similarly, mannose (10 mM), which is not transported by SGLT1, does not alter phloridzin-inhibitable ^{14}C-labeled α-D-methyl glucoside uptake. In contrast, 10 mM glucose competitively inhibited ^{14}C-labeled α-D-methyl glucoside uptake by >98%. Values are means ± SE of triplicate measurements.

activity we measured using immunoprecipitated p38 MAP kinase and an in vitro kinase assay (Fig. 9; $P < 0.05$). Thus p38 MAP kinase activity is rapidly increased after initiation of Na^+-glucose cotransport. We also examined p38 MAP kinase activation, by diphosphorylation, after cell swelling in 10% hypotonic medium, even though this stimulus did not cause cytoplasmic alkalinization (Fig. 3). p38 MAP kinase was activated after osmotic swelling of Caco-2 cells with 10% hypotonic medium in the absence of Na^+-glucose cotransport. However, this p38 MAP kinase activation occurred more slowly than that following initiation of Na^+-glucose cotransport, with a lag of 60–90 s in hypotonic medium-induced p38 MAP kinase activation relative to Na^+-glucose cotransport-induced p38 MAP kinase activation. Moreover, the maximal degree of p38 MAP kinase activation by 10% hypotonic medium (at 240 s) was only 20 ± 2% of that induced by Na^+-glucose cotransport.

Pharmacological activation of p38 MAP kinase induces cytoplasmic alkalinization. The data above show that p38 MAP kinase inhibitors can prevent NHE3-dependent cytoplasmic alkalinization after initiation of Na^+-glucose cotransport and that p38 MAP kinase activity is increased after initiation of Na^+-glucose cotransport. To test whether p38 MAP kinase activation alone could cause NHE3-dependent cytoplasmic alkalinization without Na^+-glucose cotransport, we used the chemical stressor anisomycin to activate p38 MAP kinase. Anisomycin (0.3 μM) caused a 4.3 ± 0.4-fold increase in p38 MAP kinase diphosphorylation and a 3.7 ± 0.4-fold increase in p38 MAP kinase activity. In the absence of Na^+-glucose cotransport, addition of anisomycin caused cytoplasmic alkalinization of 0.047 ± 0.006 pH unit within 120 s (Fig. 10; $P < 0.01$). S-3226 reduced anisomycin-induced cytoplasmic alkalinization to 0.001 ± 0.004 pH unit (Fig. 10; $P < 0.01$), verifying the role of NHE3 in anisomycin-induced cytoplasmic alkalinization. In contrast, 50 μM HOE-604 did not inhibit anisomycin-induced cytoplasmic alkalinization. Finally, anisomycin-induced cytoplasmic alkalinization was completely prevented by PD-169316, confirming the role of p38 MAP kinase in this alkalinization (Fig. 10; $P < 0.01$). Thus p38 MAP kinase activation is sufficient to induce NHE3-dependent cytoplasmic alkalinization, although to a slightly lesser degree than the alkalinization following initiation of Na^+-glucose cotransport.

NHE3-dependent alkalinization following Na^+-glucose cotransport is not mediated by phosphatidylinositol 3-kinase or actomyosin function. Small intestinal NHE3-dependent Na^+ absorption is acutely upregulated by epidermal growth factor (7). Inhibition of

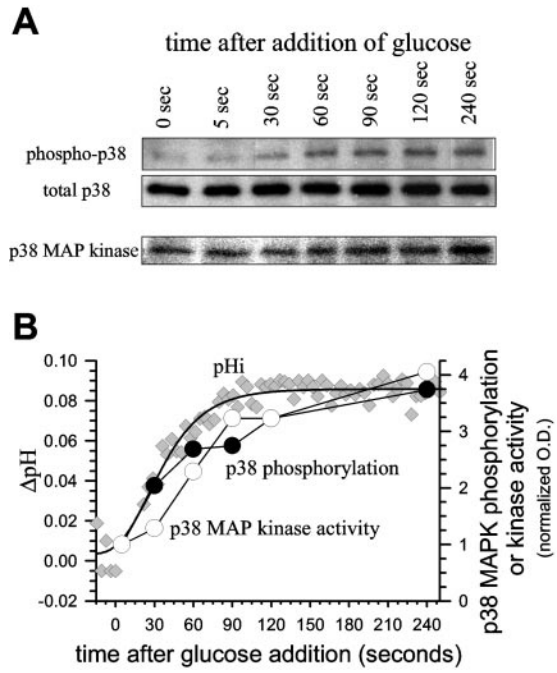

Fig. 9. p38 MAP kinase is activated after initiation of Na^+-glucose cotransport. *A*: Caco-2 cell monolayers were incubated in medium containing 25 mM mannose. At indicated times after transfer to medium containing 25 mM glucose, cells were harvested. *Top* and *middle immunoblots*: phospho-p38 MAP kinase and total p38 MAP kinase, respectively. p38 MAP kinase is rapidly phosphorylated after transfer of cell monolayers to medium containing 25 mM glucose. *Bottom immunoblot*: a phosphorylated fragment of ATF-2, a p38 MAP kinase substrate. ATF-2 was phosphorylated in an in vitro kinase reaction using p38 MAP kinase immunoprecipitated from Caco-2 lysates harvested at indicated times after transfer to medium containing 25 mM glucose. Blots are representative of 3 experiments, all with similar results. *B*: densitometric evaluation of immunoblots in *A*. Density of each band from the immunoblot for phospho-p38 MAP kinase or the phosphorylated fragment of ATF-2 was normalized to that before initiation of Na^+-glucose cotransport. Increases in phosphorylation of p38 MAP kinase (solid circles) and p38 MAP kinase activity (as assessed by ATF-2 phosphorylation, open circles) occur in parallel. Values are means of duplicate samples from the experiment shown in Fig. 5 and are representative of 3 experiments, all with similar results. Results are compared with pH_i increases after initiation of Na^+-glucose cotransport (diamonds) from a representative experiment. OD, optical density.

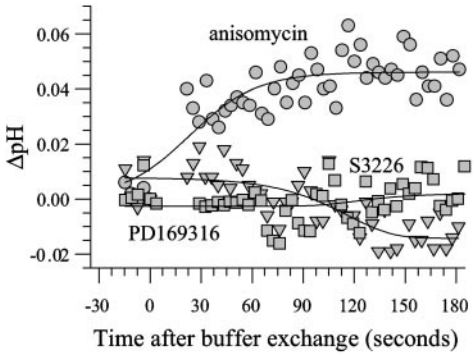

Fig. 10. Cytoplasmic alkalinization can be induced by p38 MAP kinase activation in the absence of Na^+-glucose cotransport. Addition of 0.3 μM anisomycin to Caco-2 cells in medium containing 25 mM mannose induced increases in p38 MAP kinase phosphorylation and p38 MAP kinase activity in the absence of Na^+-glucose cotransport. Addition of 0.3 μM anisomycin (circles) also caused a rapid and sustained cytoplasmic alkalinization that was quantitatively and qualitatively similar to that induced by initiation of Na^+-glucose cotransport. Addition of 0.3 μM anisomycin with 5 μM PD-169316 (inverted triangles) or 5 μM S-3226 (squares) prevented the increased pH_i induced by anisomycin, suggesting that the effect of anisomycin was due to p38 MAP kinase activation and was dependent on NHE3 activity. Values are representative of 5 experiments, all with similar results.

phosphatidylinositol 3-kinase with wortmannin prevents this epidermal growth factor-induced NHE3 activation (7). Thus it was concluded that phosphatidylinositol 3-kinase is responsible for this activation of NHE3 (7). To evaluate the potential role of phosphatidylinositol 3-kinase in NHE3-dependent cytoplasmic alkalinization after the initiation of Na^+-glucose cotransport, we tested the effect of two different phosphatidylinositol 3-kinase inhibitors, LY-294002 (50 μM) and wortmannin (100 and 500 nM), each in at least four independent trials. Neither LY-294002 nor wortmannin prevented cytoplasmic alkalinization after initiation of Na^+-glucose cotransport. Furthermore, in the absence of Na^+-glucose cotransport, epidermal growth factor (200 nM) induced only a small degree of cytoplasmic alkalinization of 0.016 ± 0.001 pH unit at 120 s ($P = 0.05$). Subsequent initiation of Na^+-glucose cotransport, in the continued presence of epidermal growth factor, resulted in typical cytoplasmic alkalinization that was not different from that induced by initiation of Na^+-glucose cotransport in the absence of epidermal growth factor. Thus, although phosphatidylinositol 3-kinase can activate NHE3 after epidermal growth factor stimulation of serum-starved NHE3-transfected Caco-2 cells (7), phosphatidylinositol 3-kinase activity does not appear to be required for Na^+-glucose cotransport-induced NHE3-dependent cytoplasmic alkalinization.

NHE3 can also be regulated by agents that disrupt actin polymerization (8) or modify myosin regulatory light chain phosphorylation (18). Therefore, we considered the possibility that actomyosin contraction could be an intermediate in NHE3 activation due to Na^+-glucose cotransport. The effects of disrupting actin structure (20 μM cytochalasin D), stabilizing actin filaments (10 μM phalloidin), inhibiting myosin light chain kinase (20 μM ML-7), inhibiting rho kinase (30 μM Y-27632), or inhibiting actomyosin contraction (10 mM 2,3-butanedione monoxime) were evaluated. In at least three independent trials, each of these treatments failed to inhibit NHE3-dependent cytoplasmic alkalinization after initiation of Na^+-glucose cotransport (data not shown). Thus these data suggest that the Na^+-glucose cotransport-dependent activation of NHE3 is independent of actomyosin function.

DISCUSSION

In the mammalian small intestine, absorption of Na^+ and glucose is essential for maintenance of fluid and electrolyte balance. However, the coordinated regulation of Na^+ absorption and Na^+-glucose cotransport has not been studied previously. Previous studies of cell volume responses after swelling induced by Na^+-glucose cotransport or hyposmotic stimuli suggest that Na^+/H^+ exchange is necessary for regulatory volume decreases (10–12). Moreover, separate studies of pH_i regulation after H^+-solute cotransport also suggest a role for Na^+/H^+ exchange in the regulation of intestinal absorption and enterocyte pH_i (19). We have developed a model of Na^+-glucose cotransport in monolayers of the human intestinal epithelial cell line Caco-2 (23), which we now use to ask whether Na^+/H^+ exchange is activated by Na^+-glucose cotransport.

On the basis of sensitivity to the Na^+/H^+ exchange inhibitor S-3226 and resistance to HOE-694, we concluded that the isoform responsible for cytoplasmic alkalinization after the initiation of apical Na^+-glucose cotransport was the apical brush-border Na^+/H^+ exchanger NHE3. However, a minority of alkalinization was not inhibitable by even 10 μM S-3226. This S-3226-resistant fraction of alkalinization is not due to NHE1 or NHE2, since S-3226 in combination with HOE-694 also failed to completely prevent cytoplasmic alkalinization after initiation of Na^+-glucose cotransport. Because our studies were performed in nominally HCO_3^--free media, it is also unlikely that this S-3226-resistant alkalinization represents HCO_3^- transport. Nonetheless, it remains a distinct possibility that, in addition to NHE3, other pH_i regulatory pathways are also activated by Na^+-glucose cotransport.

To characterize the mechanism by which Na^+-glucose cotransport leads to NHE3-dependent cytoplasmic alkalinization, we considered a variety of stimuli known to regulate NHE3. These included epidermal growth factor, phosphatidylinositol 3-kinase (7), myosin II regulatory light chain phosphorylation (18), and actin assembly (8). However, none of these signaling pathways appear to be involved in NHE3 activation after Na^+-glucose cotransport. In the case of myosin II regulatory light chain, this result is consistent with our previous data showing that NHE3 inhibition leads to reduced phosphorylation of that protein (22).

Although the buffers used in these studies were isosmotic, modest cell swelling is an established conse-

quence of Na^+-glucose cotransport in absorptive enterocytes (10). Thus we evaluated the effects of cell swelling and found that hypotonic media-induced cell volume increases alone were insufficient to trigger the NHE3-dependent pH_i increases. Despite the failure of hypotonic cell swelling alone to trigger cytoplasmic alkalinization, we also considered the possibility that p38 MAP kinase might be an intermediate in NHE3 activation after Na^+-glucose cotransport. The osmotically sensitive p38 MAP kinase has been shown to be activated by cell swelling in renal and intestinal epithelial cell lines (14, 20). We found that inhibitors of p38 MAP kinase prevented NHE3-dependent cytoplasmic alkalinization after initiation of Na^+-glucose cotransport and that initiation of Na^+-glucose cotransport led to activation of p38 MAP kinase. Nonetheless, we considered the possibility that the activation of p38 MAP kinase could be a peripheral event unrelated to the observed NHE3-dependent cytoplasmic alkalinization. However, activation of p38 MAP kinase by anisomycin in the absence of Na^+-glucose cotransport also caused NHE3-dependent cytoplasmic alkalinization, although to a quantitatively lesser degree than Na^+-glucose cotransport. Finally, we confirmed that, although hypotonic cell swelling caused p38 MAP kinase activation, this p38 MAP kinase was blunted in both response rate and magnitude relative to p38 MAP kinase activation after initiation of Na^+-glucose cotransport. We conclude that SGLT1-mediated Na^+-glucose cotransport leads to activation of p38 MAP kinase and that subsequent increases in NHE3-mediated Na^+/H^+ exchange are mediated through this p38 MAP kinase activation. The failure of hypotonic cell swelling to activate NHE3-mediated cytoplasmic alkalinization, despite activation of p38 MAP kinase, likely relates to differences in the rapidity and extent of the response. The mechanism by which SGLT1-mediated Na^+-glucose cotransport leads to activation of p38 MAP kinase is unknown. However, because intracellular Ca^{2+} signaling occurs after Na^+-glucose cotransport-induced and hypotonic media-induced cell swelling and is necessary for volume regulation in both cases (13), one possibility may be that such increases in intracellular Ca^{2+} are responsible for p38 MAP kinase activation (5, 9). Although we have not measured intracellular Na^+ directly, one might anticipate that increases in intracellular Na^+ concentration caused by Na^+-glucose cotransport and Na^+/H^+ exchange alter the driving force for Na^+/H^+ exchange. These intracellular Na^+ concentration increases could represent the compensatory mechanism that limits the magnitude of pH_i increases and establishes the new steady-state pH_i.

It is possible that the NHE3 activation we have identified after Na^+-glucose cotransport allows the coordinated activation of Na^+-absorptive pathways in vivo. Because activation of Na^+-nutrient, e.g., Na^+-glucose, cotransport signals the presence of luminal nutrients, a system where this in turn activates other absorptive pathways could be reasonably envisioned. Thus Na^+-glucose cotransport may lead to increased Na^+ absorption via NHE3, the major mechanism of Na^+ absorption in mammalian small intestine. In this manner, the initiation of Na^+-glucose cotransport could trigger a shift of the cell from a quiescent to an active state with regard to nutrient and ion absorption.

In summary, the data demonstrate NHE3 activation and pH_i regulation after the initiation of Na^+-glucose cotransport in absorptive epithelia and also suggest that p38 MAP kinase is an integral part of this signaling pathway. Thus, in addition to signaling osmotic stress, p38 MAP kinase may be, in part, responsible for the coordinated regulation of Na^+-nutrient cotransport and Na^+/H^+ exchange in absorptive enterocytes.

We are indebted to Drs. Mark Donowitz and Marshall Montrose for helpful discussion and Drs. Lucia Schuger and Judith Turner for critical review of the manuscript.

This work was supported by National Institute of Diabetes and Digestive and Kidney Diseases Grants DK-02503 and DK-56121.

REFERENCES

1. **Chow CW, Khurana S, Woodside M, Grinstein S, and Orlowski J.** The epithelial Na^+/H^+ exchanger, NHE3, is internalized through a clathrin-mediated pathway. *J Biol Chem* 274: 37551–37558, 1999.
2. **Counillon L, Scholz W, Lang HJ, and Pouyssegur J.** Pharmacological characterization of stably transfected Na^+/H^+ antiporter isoforms using amiloride analogs and a new inhibitor exhibiting anti-ischemic properties. *Mol Pharmacol* 44: 1041–1045, 1993.
3. **Hayashi M, Yoshida T, Monkawa T, Yamaji Y, Sato S, and Saruta T.** Na^+/H^+ exchanger 3 activity and its gene in the spontaneously hypertensive rat kidney. *J Hypertens* 15: 43–48, 1997.
4. **Hoogerwerf WA, Tsao SC, Devuyst O, Levine SA, Yun CH, Yip JW, Cohen ME, Wilson PD, Lazenby AJ, Tse CM, and Donowitz M.** NHE2 and NHE3 are human and rabbit intestinal brush-border proteins. *Am J Physiol Gastrointest Liver Physiol* 270: G29–G41, 1996.
5. **Ikeda M, Gunji Y, Yamasaki S, and Takeda Y.** Shiga toxin activates p38 MAP kinase through cellular Ca^{2+} increase in Vero cells. *FEBS Lett* 485: 94–98, 2000.
6. **Janecki AJ, Montrose MH, Zimniak P, Zweibaum A, Tse CM, Khurana S, and Donowitz M.** Subcellular redistribution is involved in acute regulation of the brush border Na^+/H^+ exchanger isoform 3 in human colon adenocarcinoma cell line Caco-2. Protein kinase C-mediated inhibition of the exchanger. *J Biol Chem* 273: 8790–8798, 1998.
7. **Khurana S, Nath SK, Levine SA, Bowser JM, Tse CM, Cohen ME, and Donowitz M.** Brush border phosphatidylinositol 3-kinase mediates epidermal growth factor stimulation of intestinal NaCl absorption and Na^+/H^+ exchange. *J Biol Chem* 271: 9919–9927, 1996.
8. **Kurashima K, D'Souza S, Szaszi K, Ramjeesingh R, Orlowski J, and Grinstein S.** The apical Na^+/H^+ exchanger isoform NHE3 is regulated by the actin cytoskeleton. *J Biol Chem* 274: 29843–29849, 1999.
9. **Lee SA, Park JK, Kang EK, Bae HR, Bae KW, and Park HT.** Calmodulin-dependent activation of p38 and p42/44 mitogen-activated protein kinases contributes to c-*fos* expression by calcium in PC12 cells: modulation by nitric oxide. *Brain Res Mol Brain Res* 75: 16–24, 2000.
10. **MacLeod RJ and Hamilton JR.** Volume regulation initiated by Na^+-nutrient cotransport in isolated mammalian villus enterocytes. *Am J Physiol Gastrointest Liver Physiol* 260: G26–G33, 1991.
11. **MacLeod RJ and Hamilton JR.** Activation of Na^+/H^+ exchange is required for regulatory volume decrease after modest "physiological" volume increases in jejunal villus epithelial cells. *J Biol Chem* 271: 23138–23145, 1996.

12. **MacLeod RJ and Hamilton JR.** Increases in intracellular pH and Ca^{2+} are essential for K^+ channel activation after modest "physiological" swelling in villus epithelial cells. *J Membr Biol* 172: 47–58, 1999.
13. **MacLeod RJ, Lembessis P, and Hamilton JR.** Differences in Ca^{2+}-mediation of hypotonic and Na^+-nutrient regulatory volume decrease in suspensions of jejunal enterocytes. *J Membr Biol* 130: 23–31, 1992.
14. **Niisato N, Post M, Van Driessche W, and Marunaka Y.** Cell swelling activates stress-activated protein kinases, p38 MAP kinase and JNK, in renal epithelial A6 cells. *Biochem Biophys Res Commun* 266: 547–550, 1999.
15. **Rowe WA, Lesho MJ, and Montrose MH.** Polarized Na^+/H^+ exchange function is pliable in response to transepithelial gradients of propionate. *Proc Natl Acad Sci USA* 91: 6166–6170, 1994.
16. **Schultheis PJ, Clarke LL, Meneton P, Miller ML, Soleimani M, Gawenis LR, Riddle TM, Duffy JJ, Doetschman T, Wang T, Giebisch G, Aronson PS, Lorenz JN, and Shull GE.** Renal and intestinal absorptive defects in mice lacking the NHE3 Na^+/H^+ exchanger. *Nat Genet* 19: 282–285, 1998.
17. **Schwark JR, Jansen HW, Lang HJ, Krick W, Burckhardt G, and Hropot M.** S3226, a novel inhibitor of Na^+/H^+ exchanger subtype 3 in various cell types. *Pflügers Arch* 436: 797–800, 1998.
18. **Szaszi K, Kurashima K, Kapus A, Paulsen A, Kaibuchi K, Grinstein S, and Orlowski J.** RhoA and rho kinase regulate the epithelial Na^+/H^+ exchanger NHE3. Role of myosin light chain phosphorylation. *J Biol Chem* 275: 28599–28606, 2000.
19. **Thwaites DT, Ford D, Glanville M, and Simmons NL.** H^+/solute-induced intracellular acidification leads to selective activation of apical Na^+/H^+ exchange in human intestinal epithelial cells. *J Clin Invest* 104: 629–635, 1999.
20. **Tilly BC, Gaestel M, Engel K, Edixhoven MJ, and de Jonge HR.** Hypo-osmotic cell swelling activates the p38 MAP kinase signalling cascade. *FEBS Lett* 395: 133–136, 1996.
21. **Turk E, Zabel B, Mundlos S, Dyer J, and Wright EM.** Glucose/galactose malabsorption caused by a defect in the Na^+/glucose cotransporter. *Nature* 350: 354–356, 1991.
22. **Turner JR, Black ED, Ward J, Tse CM, Uchwat FA, Alli HA, Donowitz M, Madara JL, and Angle JM.** Transepithelial resistance can be regulated by the intestinal brush border Na^+/H^+ exchanger NHE3. *Am J Physiol Cell Physiol* 279: C1918–C1924, 2000.
23. **Turner JR, Lencer WI, Carlson S, and Madara JL.** Carboxy-terminal vesicular stomatitis virus G protein-tagged intestinal Na^+-dependent glucose cotransporter (SGLT1): maintenance of surface expression and global transport function with selective perturbation of transport kinetics and polarized expression. *J Biol Chem* 271: 7738–7744, 1996.
24. **Turner JR, Rill BK, Carlson SL, Carnes D, Kerner R, Mrsny RJ, and Madara JL.** Physiological regulation of epithelial tight junctions is associated with myosin light-chain phosphorylation. *Am J Physiol Cell Physiol* 273: C1378–C1385, 1997.
25. **Watts BA III and Good DW.** Hyposmolality stimulates apical membrane Na^+/H^+ exchange and HCO_3^- absorption in renal thick ascending limb. *J Clin Invest* 104: 1593–1602, 1999.
26. **Weinman EJ, Steplock D, Wang Y, and Shenolikar S.** Characterization of a protein cofactor that mediates protein kinase A regulation of the renal brush border membrane Na^+-H^+ exchanger. *J Clin Invest* 95: 2143–2149, 1995.
27. **Wormmeester L, Sanchez de Medina F, Kokke F, Tse CM, Khurana S, Bowser J, Cohen ME, and Donowitz M.** Quantitative contribution of NHE2 and NHE3 to rabbit ileal brush-border Na^+/H^+ exchange. *Am J Physiol Cell Physiol* 274: C1261–C1272, 1998.
28. **Yun CH, Oh S, Zizak M, Steplock D, Tsao S, Tse CM, Weinman EJ, and Donowitz M.** cAMP-mediated inhibition of the epithelial brush border Na^+/H^+ exchanger, NHE3, requires an associated regulatory protein. *Proc Natl Acad Sci USA* 94: 3010–3015, 1997.